Journal of Applied Polymer Science

# Synthesis of a perfluorooctanoic acid molecularly imprinted polymer for the selective removal of perfluorooctanoic acid in an aqueous environment

**Fengmei Cao, Lei Wang, Xinhao Ren, Hongwen Sun**

Ministry of Education Key Laboratory of Pollution Processes and Environmental Criteria, Tianjin Key Laboratory of Environmental Remediation and Pollution Control, College of Environmental Science and Engineering, Nankai University, Tianjin 300071, China

Correspondence to: H. Sun (E-mail: sunhongwen@nankai.edu.cn)

**ABSTRACT:** Perfluorooctanoic acid (PFOA) contamination in the environment is a global problem. The aqueous phase is the main medium for PFOA because of its moderate solubility. Adsorption is a feasible way to remove PFOA because of its chemical and biological stability. In this study, a new type of molecularly imprinted polymer (MIP) for the selective adsorption of PFOA in aqueous solutions was synthesized by the precipitation polymerization method with PFOA as the template molecule after optimization. The adsorption kinetics and isotherms of the MIP adsorbent toward PFOA were studied, and the effects of the pH and cations on the adsorption were investigated with batch experiments. The results show that acrylamide (AAM) was the best functional monomer, and the optimal molar ratio of PFOA to AAM to ethylene glycol dimethacrylate (crosslinker) was 1:6:25. The optimized MIP adsorbent had a high affinity for PFOA, and the uptake percentage by the MIP adsorbent was 1.3–2.5 times that of the nonimprinted polymer (NIP) when PFOA existed alone. A maximum PFOA sorption capacity of 5.45 mg/g based on the Langmuir isotherm model was achieved with the MIP adsorbent. The MIP adsorbent exhibited a high selectivity for PFOA over competitive compounds (other perfluorinated alkyl carboxylic and sulfonic acids), whereas the NIP did not. Approximately 90% of the PFOA in the mixture was removed by the MIP adsorbent; this was 18 times that of the NIP. Moreover, the regenerability of the MIP adsorbent was confirmed in five sequential adsorption–desorption cycles without a significant reduction in the PFOA uptake. © 2016 Wiley Periodicals, Inc. J. Appl. Polym. Sci. **2016**, *133*, 43192.

**KEYWORDS:** kinetics; properties and characterization; recycling; separation techniques; synthesis and processing

Received 5 September 2015; accepted 7 November 2015

**DOI: 10.1002/app.43192**

## INTRODUCTION

Perfluorinated compounds (PFCs) have been commercially produced for decades and have been used in a variety of consumer and industrial applications, including surfactants,[1,2] flame retardants,[3] lubricants, and polymer additives. Recently, PFCs have raised considerable concerns because of their global distribution, notable bioaccumulation, and potential risks for human beings and ecosystems.[4–6] Perfluorooctanoic acid (PFOA) and perfluorooctane sulfonate (PFOS) are the two PFCs generating the most concern because of their frequent detection rates. In 2009, PFOS was added to the list of persistent organic pollutants under the Stockholm Convention, and its environmental concentration has been decreasing in recent years in the light of global restrictions.[7] The risk of PFOA has attracted considerable attention, and the U.S. Environment Protection Agency has classified it as a suspected carcinogen. However, PFOA is still used in many industries.[8]

The high electronegativity of the fluorine atom confers a strong polarity to the carbon–fluorine bond, and the energy of carbon–fluorine bond is among the greatest bond energies in nature.[9] As a result, PFOA can resist common biological and chemical degradation and is persistent in the environment. It has been detected in wastewater,[10] surface water,[11] ground water,[12] and even drinking water throughout the world because of its release from related products.[13] PFOA may also be directly discharged from industries, and elevated environmental PFOA concentrations have been reported in water bodies near fluorochemical factories.[14,15] Furthermore, potential precursors in wastewater influents, such as fluorotelomers, can be incompletely degraded to intermediates, including PFOA[16]; this leads to elevated PFOA concentrations in effluents.[17] Although the source, transportation, and fate of PFOA are not clearly understood, industrial and domestic wastewaters containing fluorine are considered the major source of PFOA in the environment. Thus, an effective technology for removing PFOA from aqueous

environments, particularly those industrial wastewaters containing high concentrations of PFOA, is urgently needed.

The molecular imprinting technique is an emerging technology for recognizing molecules. It can synthesize molecularly imprinted polymers (MIPs) with a high affinity and selectivity for the target chemical. MIPs have attracted considerable scientific interest, particularly in the fields of chemistry, environmental science, and biology, for use as adsorbents to remove pollutants and in solid-phase extraction,[18–20] sensors,[21,22] catalysts,[23] enzyme mimics,[24] and receptors and antibodies.[25] Three particular features make MIPs the target of extensive investigation: the striking resemblance of their binding properties (affinity and selectivity) compared to those of natural adsorbents, their unique stability, and their ease of preparation and adaptation to different fields. Recently, the molecular imprinting technique has been used increasingly in environmental fields for the selective removal or preconcentration of environmental pollutants.[26–30] However, to the best of our knowledge, only three studies have been reported on the removal of PFCs from water by MIPs, one on PFOA[31] and two on PFOS.[32,33]

In this study, we synthesized a new noncovalent imprinted polymer that could selectively adsorb PFOA with the molecular imprinting technique with acrylamide (AAM) as the monomer. The properties of the MIP adsorbent were characterized by scanning electron microscopy, Fourier transform infrared (FTIR) spectroscopy, $\zeta$ potential measurements, solid-state $^{13}$C-NMR, and Brunauer–Emmett–Teller analysis. The adsorption kinetics, isotherms, and influencing factors of the MIP adsorbent toward PFOA in the aqueous phase were studied and are discussed. Moreover, the selective recognition for PFOA and regenerability of the MIP adsorbent were evaluated.

## EXPERIMENTAL

### Materials

PFOA (98%), acrylic acid (AA) stabilized with hydroquinone methyl ether. AAM (99%), ethylene glycol dimethacrylate (EGDMA, 99%), and 2,2′-azobisisobutyronitrile were purchased from J&K Chemical Reagent Co. (Beijing, China). Monomers of 2-(trifluoromethyl) acrylic acid (TFMAA), 2-vinyl pyridine (2-Vpy), and 4-vinyl pyridine (4-Vpy) were obtained from Sigma-Aldrich (Shanghai, China). Acetone and methanol (HPLC grade) were obtained from Kangkede Reagent Co. (Tianjin, China). The reagents stabilized with hydroquinone methyl ether were treated with distillation under reduced pressure to remove the inhibitor, and 2,2′-azobisisobutyronitrile was recrystallized before use. Perfluorobutane sulfonate (PFBS; purity = 98%), perfluorododecanoic acid (PFDoA; purity = 95%), and PFOS (purity = 98%) were supplied by Sigma-Aldrich Chemical (Milwaukee, WI). Perfluoropentanoic acid (PFPeA) was obtained from Tokyo Kasei (Japan), and perfluorohexanoic acid (PFHxA; purity = 98%), perfluoroheptanoic acid (PFHpA; purity = 98%), and perfluoroundecanoic acid (PFUnA; purity $\geq$ 96%) were products of Matrix Scientific. PFOA (purity = 98%) was supplied by Strem Chemicals (France). Perfluorononanoic acid (PFNA; purity = 98%), perfluorodecanoic acid (PFDA; purity = 98%), and perfluorohexane sulfonate (PFHxS; purity = 98%) were purchased from Fluorochem (United Kingdom). The internal standard $^{13}C_8$–PFOA (purity = 99%) used in the internal calibration for high-performance liquid chromatography (HPLC) with tandem mass spectrometric (MS/MS) analysis was purchased from Wellington Laboratories (Guelph, Ontario, Canada). All other chemicals were analytical reagent grade, and Milli-Q water was used in this study. Solutions of 0.1 m*M* NaOH and HCl were used to adjust the pH values.

### Preparation of the MIP with the Precipitation Method

The PFOA–MIP adsorbent was prepared with the precipitation method.[34] Different polymers were prepared with different monomers and molar ratios of PFOA/AAM/EGDMA to obtain a good adsorbent. The template molecule, PFOA (0.0414 g, 0.1 mmol), was dissolved in 10 mL of acetone in a 50-mL conical flask, and then, the functional monomer, AAM (0.0426 g, 0.6 mmol), or an appropriate amount of another monomer was added. During the optimization of the functional monomers, the PFOA/AAM/EGDMA molar ratio was set at 1:4:20. The mixture was stirred for 3 h at room temperature to ensure thorough mixing and to allow for sufficient interactions between the functional groups in the monomer molecules and the carboxylic group in the PFOA molecules. Then, prepolymerization was initiated by the addition of 0.010 g of the initiator 2,2′-azobisisobutyronitrile. The mixture was degassed under sonication for 10 min; this was followed by nitrogen purging for 10 min. Then, 470 $\mu$L (2.5 mmol) of EGDMA was added to the glass vial, which was then incubated in a water bath at 60°C with magnetic stirring at 200–300 rpm. The reaction lasted for 12 h. The obtained polymer particles were washed with methanol–acetic acid (6:1 v/v) under sonication to remove the template and then washed with Milli-Q water until the pH of the supernatant was close to that of the Milli-Q water. Finally, the polymer particles were dried in a vacuum oven at 60°C overnight. As a reference polymer, a nonimprinted polymer (NIP) was synthesized and treated under the same procedure without the addition of the template PFOA during the synthesis process.

### Characterization of the MIP and NIP

FTIR data were obtained with a Tensor 27 spectrometer (German Bruker Co., Kleve, Germany) in the wave-number range 400–4000 cm$^{-1}$. Solid-state $^{13}$C-NMR MAS spectroscopy measurements were performed at 400 MHz on a Varian Infinityplus-400 spectrometer (Varian, Palo Alto, CA) equipped with 2.5-, 4.0-, and 7.5-mm MAS probes. The specific surface area and porosity were measured with an ASAP 2000 instrument (Micromeritics) on the basis of the nitrogen adsorption–desorption analysis of the Brunauer–Emmett–Teller multipoint adsorption isotherm (maximum experimental error < 1%). The $\zeta$ potentials of the MIP and NIP in water solutions at various pH levels were determined with a JS94H microscopic–electrophoresis instrument (Zhongchen Digital Technical Apparatus Co., Shanghai, China).

### Batch Adsorption Experiments

Batch adsorption experiments were conducted to examine the adsorption kinetics, adsorption isotherms, and effects of the pH and ionic strength on adsorption. To determine the adsorption kinetics, 10 mg of the MIP adsorbent was added to polypropylene (PP) tubes containing 50 mL of a 20 $\mu$g/L PFOA solution. The tubes were shaken in a shaker operated at 200 rpm and 20°C. The kinetic test lasted for 48 h, and three triplicate tubes were taken

out at designated intervals (i.e., 2, 4, 6, 8, 10, 12, 24, 36, and 48 h). The sorbents were filtered, and the concentration of PFOA in the residual solution was determined by liquid chromatography with tandem mass spectrometric (LC/MS/MS).

On the basis of the results of the kinetic test, an equilibrium time of 12 h was selected for the isotherm experiment. Ten milligrams of the MIP adsorbent was added to 50-mL solutions containing certain amounts (5 $\mu$g/L to 1.0 mg/L) of PFOA at pH 5.0 in PP tubes, and the tubes were shaken for 12 h under the same conditions as used in the kinetic test. To determine the impacts of the influencing factors on the adsorption efficiency, the adsorptions of 20 and 100 $\mu$g/L PFOA were examined at initial pH values ranging from 2.0 to 10.0, and the adsorptions of 100 $\mu$g/L PFOA were examined in NaCl or $CaCl_2$ solutions with concentrations ranging from 0 to 500 mmol/L. The other conditions were the same as described previously. All of the adsorption experiments were conducted in triplicate, and the data presented are the average with relative standard deviations.

### Selective Recognition Experiment

To ensure the selective recognition of the PFOA–MIP for PFOA and other PFCs (i.e., PFPeA, PFHxA, PFHpA, PFNA, PFDA, PFUnA, PFDoA, PFBS, PFHxS, and PFOS), 10 mg of the PFOA–MIP and NIP, respectively, were added to 50-mL PP tubes, each of which contained 50 mL of solution with 20 $\mu$g/L PFOA and the same concentration of the other PFCs (20 $\mu$g/L). The experiments were carried out on a shaker at room temperature for 12 h under the same conditions as used in the isotherm experiments.

### Desorption and Regeneration Experiment

The MIP adsorbent with sorbed PFOA was regenerated by shaking with a methanol–acetic acid solution (6:1 v/v) for 12 h in a shaker, which was operated under the same conditions as used in the adsorption experiments. Then, it was rinsed with Milli-Q water until the pH of the supernatant was close to that of the Milli-Q water. The regenerated PFOA–MIP was then reused for the next adsorption experiment. The adsorption–desorption cycles were repeated five times under the same conditions.

### LC–MS/MS Analysis

PFOA and the other competing PFCs were measured with an Acquity ultra-performance liquid chromatography tandem mass spectrometry (UPLC) system (Waters, Milford, MA) coupled with a triple-quadrupole mass spectrometer (Waters Micromass, Manchester, United Kingdom). This system was equipped with a Waters 2777C sample manager and an Acquity binary solvent manager. The PFCs were determined with an orthogonal Z-spray–electrospray ionization source in the negative-ion mode. An Acquity UPLC bridged ethylsiloxane/silica hybrid (BEH) $C_{18}$ column (2.1 $\times$ 50 $mm^2$, 1.7 $\mu$m; Waters Micromass) was used. The details of the analysis were provided in our previous publication.[17]

### Data Analysis

The kinetic data were analyzed with pseudo-first-order rate and pseudo-second-order rate equations, expressed in eqs. (1) and (2), respectively:

$$q_t = q_e - q_e e^{-k_1 t} \quad (1)$$

$$q_t = \frac{k_{2q_e^2 t}}{1 + k_2 q_e t} \quad (2)$$

where $q_e$ and $q_t$ are the amounts of PFOA adsorbed onto the adsorbent (mg/g) at equilibrium and at time $t$ (h), respectively, and $k_1$ and $k_2$ are the pseudo-first-order rate constant ($h^{-1}$) and pseudo-second-order rate constants (g $mg^{-1}$ $h^{-1}$), respectively.[35,36]

The adsorption isotherms were fitted to the Langmuir and Freundlich isotherm models, respectively. The nonlinear form of the Langmuir isotherm model is given as follows:

$$q_e = \frac{q_m C_e}{\frac{1}{K_L} + C_e} \quad (3)$$

where $q_m$ is the theoretical maximum monolayer capacity (mg/g), $C_e$ is the equilibrium concentration (mg/L), and $K_L$ is the Langmuir constant, which reflects the affinity of the active sites toward the adsorbate molecules (L/mg).

The dimensionless separation factor ($R_L$), which is used to predict the favorability of an adsorbent, was calculated with the following equation[37]:

$$R_L = \frac{1}{1 + c_m K_L} \quad (4)$$

where $c_m$ is the maximal initial concentration of the analyte (mg/L) and $R_L$ values within 0–1.0 represent an adequate isotherm model.

The nonlinear form of the Freundlich isotherm model is given in eq. (5):

$$q_e = K_F C_e^{\,n} \quad (5)$$

where $K_F$ and $n$ are the Freundlich adsorption constant [(mg/L)/(mg/L)$^n$] and isotherm nonlinearity factor, respectively. These terms are related to the adsorption capacity and adsorption favorability, respectively. All of the data were analyzed by Origin 8.0 software.

## RESULTS AND DISCUSSION

### Optimization of the Preparation of the PFOA–MIP

**Optimization of the Functional Monomer.** Because functional monomers directly affect the imprinting efficiency,[38] the type of functional monomer must be optimized. In this study, we checked for several functional monomers that are commonly used for the synthesis of MIPs, including AA, AAM, 2-Vpy, and 4-Vpy. The TFMAA that was proposed by Matsui *et al.*[39] to provide additional fluorine–fluorine interaction was also included in this study. The optimized conformations of PFOA and the five functional monomers are shown in Figure 1. The uptake percentages of PFOA onto the polymers synthesized by different monomers are shown in Figure 2; they followed the order AAM $\approx$ 2-Vpy $\approx$ 4-Vpy $>$ TFMAA $>$ AA. The polymer synthesized by AA showed the weakest adsorption for PFOA; this may have been due to the electrostatic repulsion between the two carboxylic groups in AA and PFOA. The substitution with trifluoromethane onto AA (TFMAA) enhanced the affinity of the polymer toward PFOA considerably because of the fluorine–fluorine interaction.[39] However, the adsorption capacity of

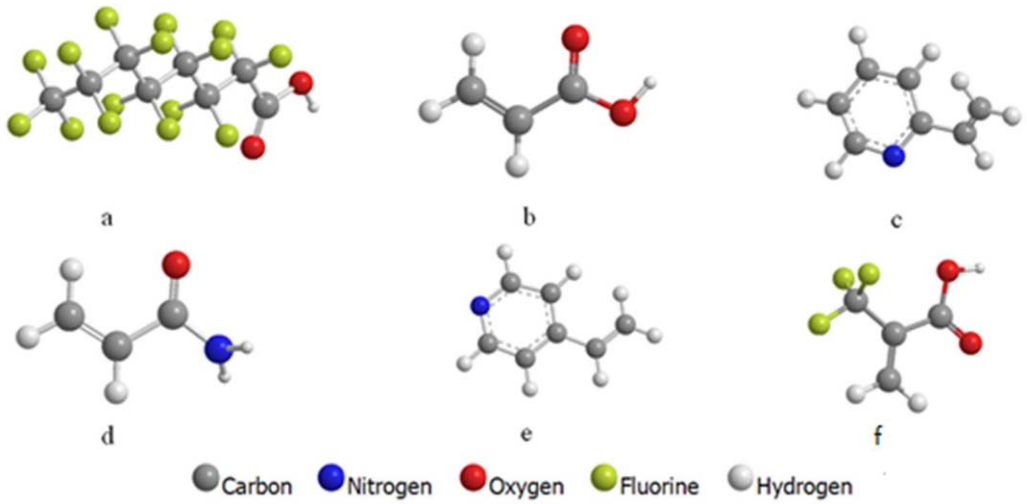


**Figure 1.** Structures of (a) PFOA and the monomers (b) AA, (c) 2-Vpy, (d) AAM, (e) 4-Vpy, and (f) TFMAA. [Color figure can be viewed in the online issue, which is available at wileyonlinelibrary.com.]

TFMAA toward PFOA was still considerably lower than those of the polymers synthesized by the other three monomers (AAM, 2-Vpy, and 4-Vpy). Among the three MIP materials, the MIP synthesized by AAM showed the highest adsorption capacity, possibly because of the hydrogen bonding between -C(O)$NH_2$ in AAM and -C(O)$O^-$ in PFOA. The high adsorption capacities of the MIPs synthesized from 2-Vpy and 4-Vpy could have resulted from the interaction of electron transfer from the pyridine ring in Vpy to the electropositive C in the carboxylic group of PFOA. Because of the toxicity of 2-Vpy and 4-Vpy, which can cause sensitization by inhalation and skin contact, the functional monomer of AAM was used as the functional monomer in the following experiments.

**Optimization of the Template/Monomer/Crosslinker Ratio.** The template/monomer/crosslinker ratio is one of the key parameters when one considers possible interactions involved inside the polymer matrix.[40] The amount of template and functional monomer can significantly affect their specific interactions. When there is an insufficient amount of crosslinker, the crosslinking reaction will not be complete; in contrast, an excessive amount of crosslinker will lead to excessive crosslinking, which is unfavorable for the removal of the template and subsequent application.[38,41] In this study, MIPs with different template/monomer/crosslinker ratios were synthesized on the basis of the ratios currently used in the literature; these are denoted as MIP1–MIP9 (Table I). The uptake percentage of PFOA onto the MIPs increased as the ratio of PFOA to AAM increased from 1:2 to 1:6 at a fixed crosslinker concentration of 2.5 mmol/L, with a maximum uptake percentage of 91.0% achieved at a PFOA/AAM ratio of 1:6. The PFOA uptake percentages decreased sharply to 86.4 and 82.0% when the PFOA/AAM ratios increased further to 1:8 and 1:10, respectively. This phenomenon was explained by the sufficient H bonds between PFOA and AAM achieved within an optimum ratio range. Then, the PFOA/AAM ratio was fixed at 1:6, and the amount of crosslinker was varied. No significant changes in the PFOA uptake percentage were found when the PFOA/EGDMA ratio

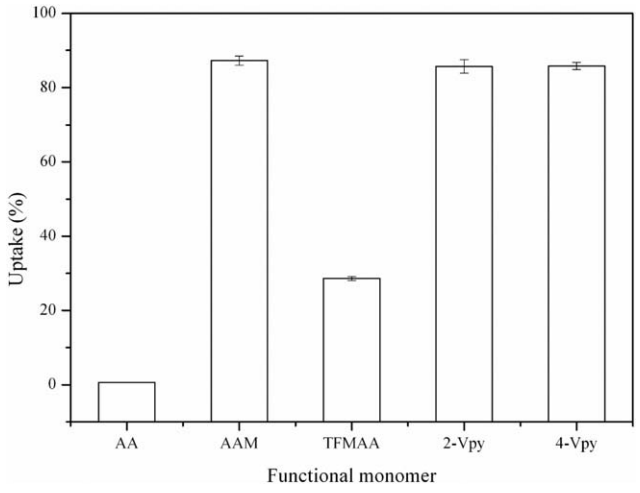


**Figure 2.** Effects of the functional monomer on the uptake percentage of PFOA by the corresponding polymer.

**Table I.** Ratios of the Template to the Monomer and Crosslinker and the Adsorption Efficiency of PFOA by the Corresponding Polymers

| Polymer | PFOA (mmol) | AAM (mmol) | EGDMA (mmol) | Uptake (%) | RSD (%) |
|---|---|---|---|---|---|
| MIP1 | 0.1 | 0.2 | 2.5 | 73.4 | 3.12 |
| MIP2 | 0.1 | 0.4 | 2.5 | 88.4 | 1.06 |
| MIP3 | 0.1 | 0.6 | 2.5 | 91.0 | 2.48 |
| MIP4 | 0.1 | 0.8 | 2.5 | 86.4 | 1.98 |
| MIP5 | 0.1 | 1.0 | 2.5 | 82.0 | 5.12 |
| MIP6 | 0.1 | 0.6 | 1.0 | 59.8 | 2.63 |
| MIP7 | 0.1 | 0.6 | 1.5 | 89.2 | 4.32 |
| MIP8 | 0.1 | 0.6 | 2.0 | 88.7 | 2.85 |
| MIP9 | 0.1 | 0.6 | 3.0 | 60.4 | 2.51 |

The MIP1–MIP9 adsorbents were synthesized with different PFOA/AAM/EGDMA ratios via the precipitation polymerization method, RSD is the relative standard deviation.

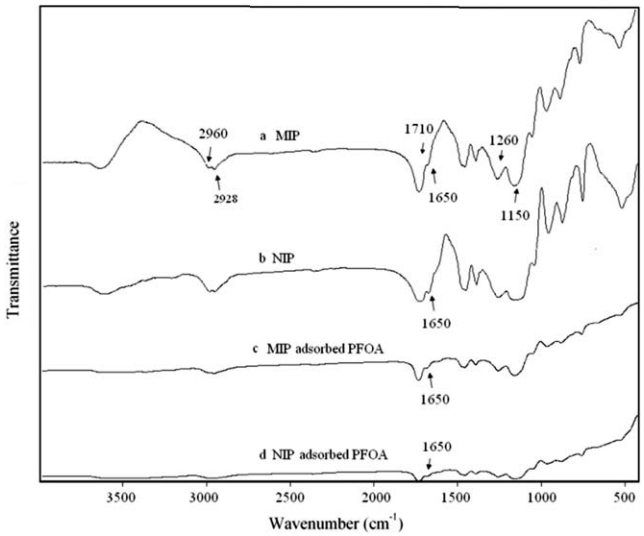


**Figure 3.** FTIR spectra of the MIP and NIP adsorbents before and after interaction with PFOA.

was changed from 1:15 to 1:20; in contrast, the uptake percentages of PFOA were low at PFOA/EGDMA ratios of 1:10 and 1:30 because there was not sufficient crosslinking to form plentiful cavities with favorable conformations at the low crosslinker level and the binding sites were partially covered because of excessive crosslinking at the high crosslinker level.[38] Hence, a ratio of 1:6:25 was used as the optimum template/monomer/crosslinker ratio in the preparation of the PFOA–MIP.

### Characterization of the MIP and NIP

**FTIR Spectra of the Particles.** The FTIR spectra of the MIP and NIP adsorbents before and after interaction with PFOA are shown in Figure 3. As shown by the FTIR spectra of the MIP, the main absorption bands were at 2960 and 2928 $cm^{-1}$ (C—H stretching vibrations of methyl and methylene), 1650 $cm^{-1}$ (C═N in AAM), and 1710, 1260, and 1150 $cm^{-1}$ (C═O symmetric and asymmetric stretching vibrations of EGDMA).[42] All of these bands proved that the MIP material had plentiful functional groups; this endowed it with the ability to bind PFOA with specific interactions. With regard to the spectra of the MIP with adsorbed PFOA, the intensity of all of the peaks decreased considerably. The peak of C═N at 1650 $cm^{-1}$ nearly disappeared; this indicated the existence of an H-bond interaction between the MIP and PFOA. In addition, the major peaks of the NIP had a similar location and appearance as those of the MIP; this indicated that the template molecules were completely removed from the polymer. The NIP with adsorbed PFOA also had similar a spectrum to that of the MIP with adsorbed PFOA. This suggested that NIP could also interact with PFOA through H bonding. The primary advantage of the MIP over the NIP was the imprinted cavities, which provided an optimum conformation that enhanced the affinity and selectivity for the target compound.

**Solid-State $^{13}$C-NMR MAS Spectra.** The solid-state $^{13}$C-NMR MAS spectra of the MIP and NIP materials before and after interaction with PFOA are shown in Figure 4. The main resonances were at 20–50 ppm (methyl and methylene groups of EGDMA), 63.1 ppm (ether of EGDMA), and 160–180 ppm [C═O of EGDMA and $C(O)NH_2$ of AAM].[41] There was no clear difference between the MIP and NIP. After the interaction with PFOA, the intensity of the typical peaks decreased considerably, particularly that of the peak at 177 ppm, which indicated that both the MIP and NIP synthesized by AAM could interact with PFOA through H bonding. Again, the advantage of the MIP over the NIP was due to conformation differences not the different chemical groups.

**Morphological Observation.** To further elucidate the microlevel mechanism of the imprinting effect, morphological studies were conducted on the MIP and NIP materials (Figure 5). The shapes of the MIP and NIP were both regular flakes. The diameters of the MIP and NIP particles were approximately 80 and 120 nm, respectively. The specific surface area and pore volume of the polymers are shown in Table II. The NIP had a smaller surface area and total pore volume than the MIP; this indicated that the MIP had a larger surface area because of imprinting. Hence, the MIP was smaller and had a larger surface area than the NIP; this was favorable for the adsorption of the target

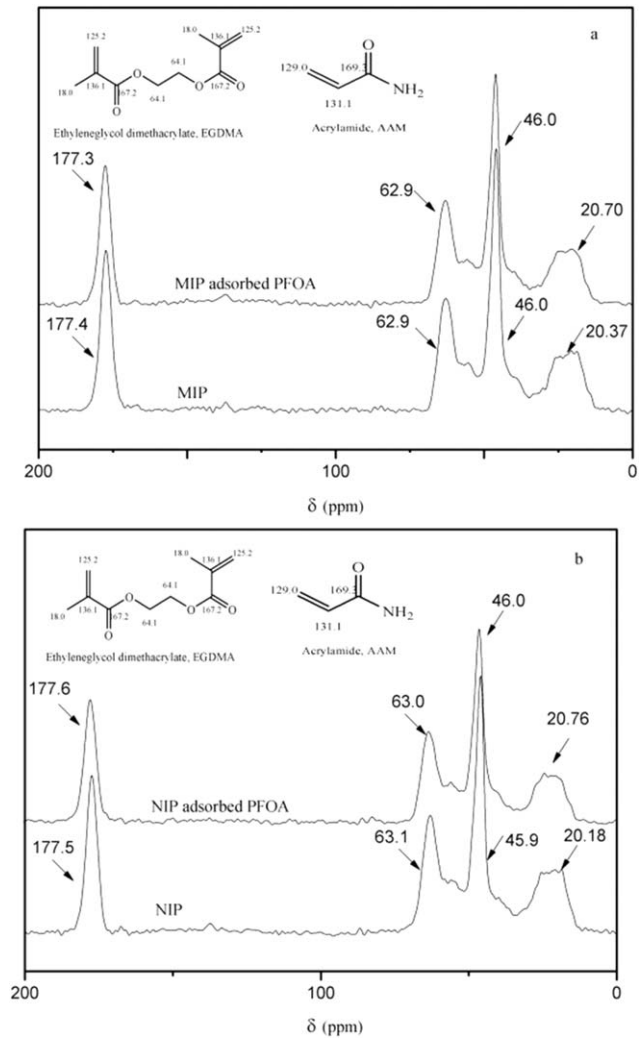


**Figure 4.** Solid-state $^{13}$C-NMR spectra of the (a) MIP and (b) NIP adsorbents before and after interaction with PFOA.

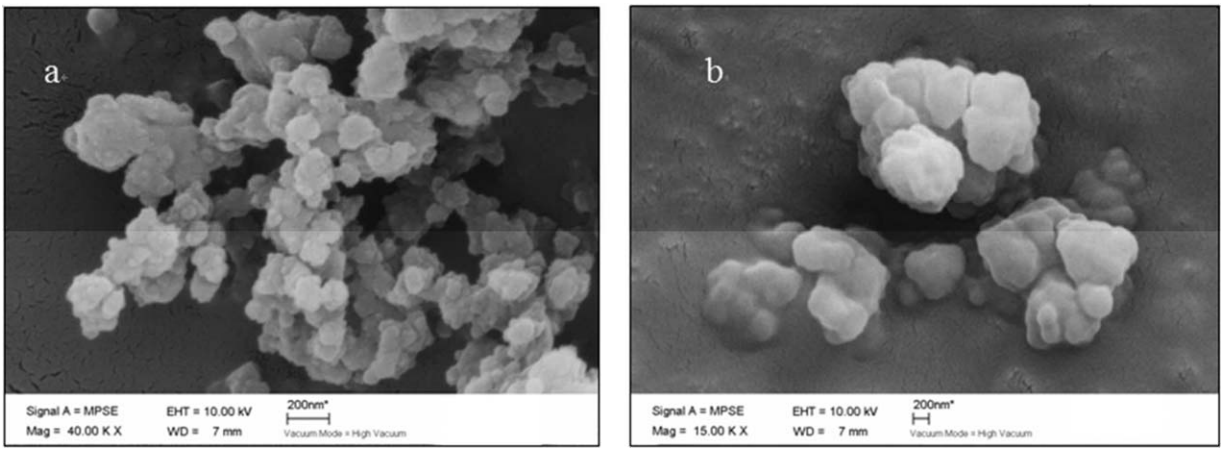


**Figure 5.** Scanning electron microscopy images of the (a) MIP and (b) NIP adsorbents.

organic contaminant. However, the larger surface area was not the only reason for the greater adsorption capacity of the MIP. The greater capacity of the MIP and its selectivity for PFOA were more significantly caused by the result of the imprinted cavities.

**ζ Potentials of the MIP and NIP.** Figure 6 shows the pH dependence of the ζ potentials of the MIP and NIP materials. The zero-charge points of the MIP and NIP were at pH values 2.49 and 2.60, respectively, which means that the MIP was positively charged at pHs of less than 2.49 and negatively charged at pHs of more than 2.49. In contrast, the NIP was positively charged at pHs of less than 2.60 and negatively charged at pHs of more than 2.60.

### Adsorption Kinetics

To describe the kinetics of the adsorption process, a pseudo-first-order model and pseudo-second-order model were used to fit the experimental data (Figure 7). In the first 8 h, the adsorption was rapid for both the MIP and NIP. Then, it became gradual and reached apparent equilibrium after 10 h. The maximum adsorption of the MIP for PFOA reached 58.9 μg/g after 12 h; this was higher than the 22.5 μg/g reached for the NIP adsorbents. This suggested a good imprinting effect of the MIP adsorbent.

The kinetic rate constants of adsorption obtained from the linear regression correlation of the kinetic models are listed in Table III. The pseudo-first-order kinetic model yielded a better fit than the pseudo-second-order kinetic model, especially for the MIP adsorbent based on the correlation coefficients. Moreover, the calculated values obtained from the pseudo-first-order kinetic model ($q_{e,cal}$'s) were closer to the experimental values ($q_{e,exp}$'s) than those obtained from the pseudo-second-order kinetic model. In the pseudo-first-order kinetic model, the kinetic rate constant was directly proportional to the concentration of adsorbates; this represented a fast adsorption process. In the pseudo-second-order model, the kinetic rate constant is related to the square of the adsorbate concentration; this suggests that the adsorption kinetics are controlled by multiple processes, including the rate-limiting step.[35,43] Moreover, the adsorption mechanisms may change with the adsorbate concentration.[44] In the kinetic experiment, a PFOA concentration of 20 μg/L was used; this was relatively low compared to those used in the isotherm experiment. This may have been the main reason that the adsorption kinetics followed a fast kinetic model.

**Table II.** Comparison of the MIP and NIP Based on Nitrogen Adsorption–Desorption Analysis

| Polymer | Surface area ($m^2$/g) | Total pore volume ($cm^3$/g) | Average pore diameter (nm) |
|---|---|---|---|
| MIP | 12.7 | 0.056 | 17.5 |
| NIP | 4.34 | 0.018 | 16.5 |

The MIP was made with a PFOA/AAM/EGDMA ratio of 1:6:25, and the NIP lacked PFOA. These definitions also apply to Table III, IV and Figures 3–12.

### Adsorption Isotherms

Adsorption isotherms can provide information on how the adsorbate molecules are distributed onto the adsorbent. In this study, two common isotherm models were used to analyze the equilibrium data (Figure 8). The isotherm parameters obtained

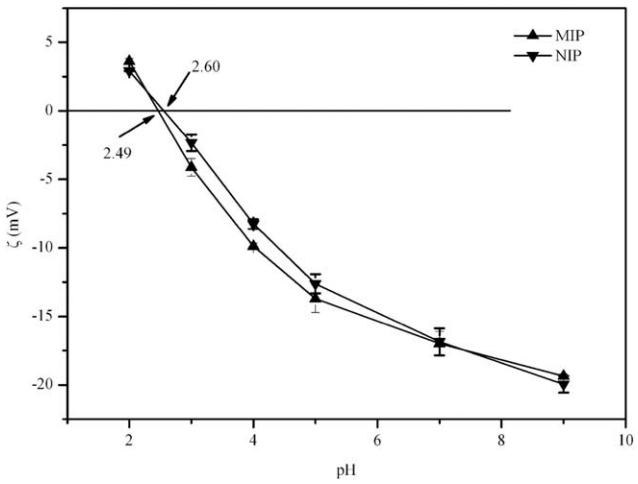


**Figure 6.** ζ potentials of the MIP and NIP adsorbents at different pH values.

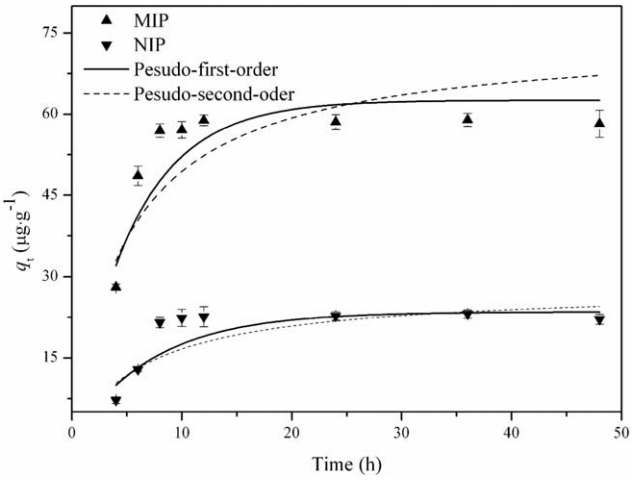


**Figure 7.** Comparison of the kinetics of the adsorption of PFOA onto the MIP and NIP adsorbents.

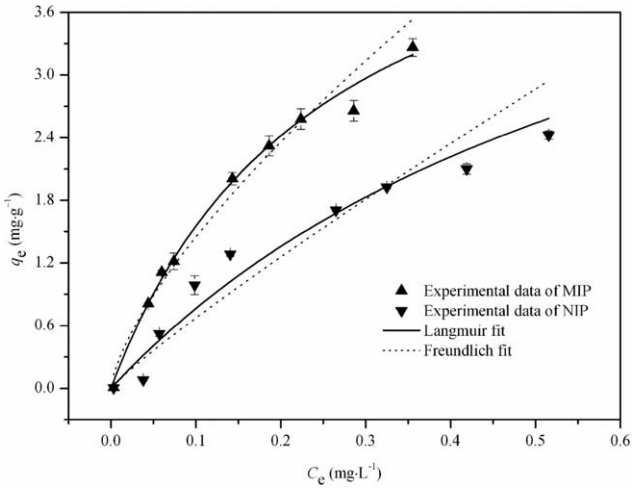


**Figure 8.** Comparison of the Langmuir and Freundlich isotherm models for PFOA adsorption onto the MIP and NIP adsorbents.

from nonlinear analysis are presented in Table IV. As illustrated in Figure 8, with increasing $C_e$ of PFOA, $q_e$ increased rapidly at first and then increased more gradually. Both the Langmuir and the Freundlich isotherm fit the isotherm data well, and the Langmuir isotherm model yielded a better fit on the basis of the slightly higher correlation coefficients ($R^2$'s) of 0.993 and 0.983 for the MIP and NIP, respectively, as compared to those of the Freundlich isotherms (Table IV). In addition, the values of $R_L$ were between 0 and 1.0; this represented the favorable adsorption conditions. Both the Langmuir and Freundlich models represent specific interactions[28,45]; this was in accordance with the previous conclusion that H bonds existed for the adsorption of PFOA onto both the MIP and NIP.

The maximum PFOA adsorption capacity ($q_m$) by the MIP was 5.45 mg/g according to the Langmuir model, whereas the corresponding value for the NIP was 5.04 mg/g (Table IV). The corresponding values in molar amounts were 13.1 and 12.1 μmol/g for the MIP and NIP materials, respectively. Comparisons with other imprinted and nonimprinted adsorbents were performed. For example, maximum PFOA adsorption capacities of 0.30 and 0.42 mmol/g were reported for powder-activated carbon and granular-activated carbon, respectively.[43] Recently, a new MIP adsorbent was developed to adsorb PFOA with β-cyclodextrin, and a $q_m$ of 2.60 mmol/g was achieved.[31] The adsorption capacity of AAM–PFOA was slightly lower, but it had a higher selectivity for PFOA, as shown in the following selectivity adsorption study. Hence, the adsorbent developed in this study by molecular imprinting technology is a promising adsorbent for PFOA removal from the aqueous phase.

### Influencing Factors

**Effect of the pH.** The effect of the pH on the adsorption capacity was investigated for a wide pH range from 2.0 to 10.0 with initial PFOA concentrations of 20 and 100 μg/L (Figure 9). The adsorption of PFOA was found to be pH-dependent. The adsorption capacity remained constant at pH values below 4.0 and decreased with increasing pH in the range from 4.0 to 10.0. The adsorption amount decreased from 89.1 to 13.8 μg/g for the 20 μg/L (initial concentration) PFOA solution and from 448 to 166 μg/g for the 100 μg/L (initial concentration) PFOA solution. The uptake percentage also decreased significantly with increasing pH from over 80% to approximately 20%.

Because of the low p$K_a$ value (ca. 2.5) of PFOA,[46] PFOA exists as an anion in neutral solutions. According to the ζ potential of the MIP adsorbent (Figure 6), the surface charge of the MIP was also negative under neutral conditions. Hence, electrostatic repulsion may have taken place between the negatively charged PFOA–MIP and the PFOA anion at high pH values. When the pH value was not high (2.0–4.0), the electrostatic repulsion did not exert a significant effect on PFOA adsorption, and the binding affinity between the target PFOA molecules and imprinted sites on the MIP adsorbent was the main driving force for the adsorption. The dissociation of PFOA became complete with increasing pH, and over 99% of the PFOA molecules existed as anions at pH values over 4.5. Consequently, the electrostatic repulsive interactions between PFOA and the MIP adsorbent became stronger; this counteracted part of the binding affinity. Hence, the adsorption capacity of PFOA decreased sharply with increasing pH. The sorption of PFOS and PFOA to natural

**Table III.** Adsorption Kinetic Parameters for the Adsorption of PFOA onto the MIP and NIP Adsorbents

| | Pseudo-first-order | | | | Pseudo-second-order | | | |
|---|---|---|---|---|---|---|---|---|
| Adsorbent | $q_{e,exp}$ (μg/g) | $q_{e,cal}$ (μg/g) | $k_1$ (h$^{-1}$) | $R^2$ | $q_{e,exp}$ (μg/g) | $q_{e,cal}$ (μg/g) | $k_2 \times 10^{-3}$ (g mg$^{-1}$ h$^{-1}$) | $R^2$ |
| MIP | 58.9 | 63.5 | 0.176 | 0.852 | 58.9 | 76.7 | 2.31 | 0.766 |
| NIP | 22.5 | 22.3 | 0.0981 | 0.996 | 22.5 | 28.2 | 3.33 | 0.995 |

**Table IV.** Adsorption Isotherm Constants for PFOA Adsorption onto MIP and NIP Adsorbents

| | Langmuir equation | | | | Freundlich equation | | |
|---|---|---|---|---|---|---|---|
| Adsorbent | $K_L$ [(mg/L)/(mg/L)$^n$] | $q_m$ (mg/g) | $R_L$ | $R^2$ | $K_F$ (mg/g) | $n$ | $R^2$ |
| MIP | 3.99 | 5.45 | 0.413 | 0.993 | 7.31 | 0.703 | 0.973 |
| NIP | 1.45 | 5.04 | 0.572 | 0.983 | 5.34 | 0.899 | 0.974 |

sediments and kaolinite at neutral pH was lower than those at a low pH value.[47] A similar result of the effect of pH was also reported for the adsorption of PFOS onto chitosan-based MIP adsorbents.[33]

**Effect of the Ionic Strength.** Inorganic salts are abundant in natural water environments. In this study, the adsorption of PFOA onto the MIP adsorbent was measured under various concentrations of NaCl and $CaCl_2$ to assess the effect of the ionic strength on the adsorption capacity of the MIP (Figure 10). The amount of PFOA adsorbed on the MIP did not change significantly when the $Na^+$ and $Ca^{2+}$ concentrations increased from 10 to 100 mmol/L. However, the amount of adsorption increased significantly as the $Na^+$ and $Ca^{2+}$ concentrations increased from 100 to 500 mmol/L. The effect of $Ca^{2+}$ was greater than that of $Na^+$. One possible reason for the enhanced PFOA adsorption was the salting-out effect. Such a salting-out effect played a significant role in the sorption process of PFOS, especially at high salt concentrations.[33] However, the water solubility of PFOA was extremely high (3.4 g/L),[48] and a significant salting-out effect was not expected. More importantly, the cations could neutralize the negative charge on both the adsorbent and PFOA molecules. Hence, the electrostatic repulsion was reduced. Moreover, the divalent $Ca^{2+}$ acted as a bridge between the negatively charged adsorbent and PFOA molecules;[49] this explained the greater effect of $Ca^{2+}$ compared to $Na^+$. The enhanced PFOA removal at high ionic strength will allow this technology to be used in the treatment of wastewaters with high salinity.

**Adsorption Selectivity**

To demonstrate the feasibility of the MIP adsorbent to selectively recognize the template molecule in a mixture, the adsorption of PFOA in the presence of some other PFCs was checked for possible interference in PFOA adsorption by PFOA–MIP and NIP (Figure 11). The PFCs included seven perfluoroalkyl carboxylic acids (i.e., PFPeA, PFHxA, PFHpA, PFNA, PFDA, PFUnA, and PFDoA) and three perfluoroalkane sulfonic acids (i.e., PFBS, PFHxS, and PFOS).

The adsorption capacities of the PFOA–MIP for the PFCs were considerably higher than those of the NIP. This suggested that imprinting process created cavities that had favorable conformations for the specific interactions. For both the MIP and NIP, it was easier for the PFCs with longer chains to be adsorbed onto the adsorbents than their shorter chain analogs. This trend was due to the greater hydrophobicity of the longer chain analogs. In the mixture, the uptake percentage of PFOA adsorbed by MIP was approximately 90.0%; this was approximately 18 times that of the NIP. This again showed the advantage of the MIP. When PFOA existed alone, the adsorption capacity of the MIP was only 1.3–2.5 times that of the NIP. In the mixture, the adsorption of PFOA onto the NIP was prohibited because of the competition of other PFCs, whereas the MIP still maintained a high uptake percentage for PFOA because of its high selectivity. The uptake percentages of the MIP for other perfluoroalkyl carboxylic acids ranged from 4.85 to 29.8%, whereas those for perfluoroalkane sulfonic acids ranged from 3.85 to 51.9%. Among the tested competitive PFCs, PFOS had the

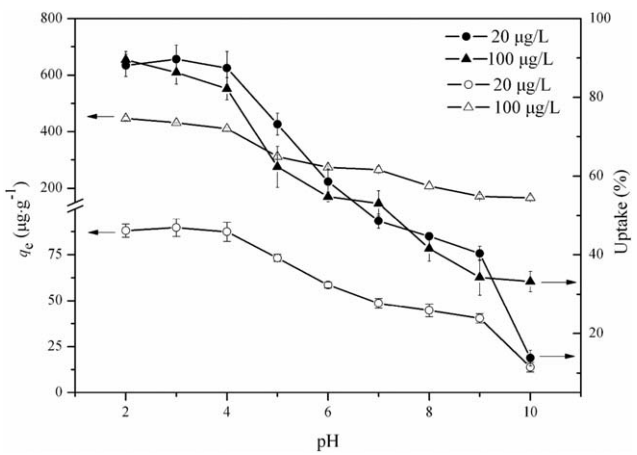


**Figure 9.** Effect of pH on the adsorption of PFOA onto the MIP adsorbent.

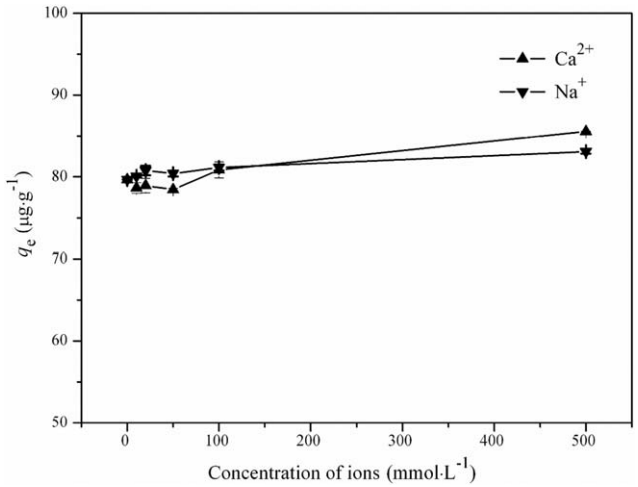


**Figure 10.** Effect of the ionic strength on the adsorption of PFOA onto the MIP adsorbent.

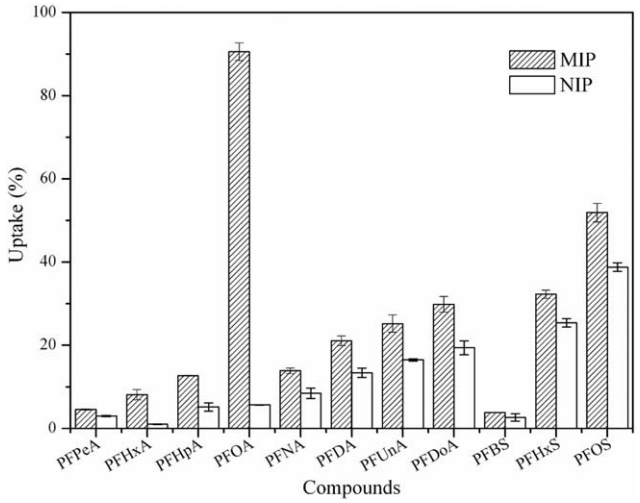


**Figure 11.** Comparison of the adsorption capacity of PFOA with other PFCs (equivalent by weight) on the MIP and NIP adsorbents.

highest uptake percentage because PFOS contains eight carbon atoms and has a similar structure to that of PFOA. The other reason for the higher uptake percentage of PFOS compared to PFHpA and PFNA, which also have molecular sizes similar to that of PFOA, was the relatively low solubility of PFOS (570 mg/L),[50] which is beneficial for hydrophobic partition. For the NIP, there were no imprinted cavities, and the functional sites of AAM in the polymer network were arranged in a disorderly manner; this accounted for its low sorption affinity. All of the experimental data demonstrated that the MIP adsorbent had excellent recognition ability and a high selectivity for PFOA in a complex environment.

### Desorption and Regeneration

Desorption and regeneration studies are important for MIP applications. In the desorption and regeneration experiments, the regenerated MIP adsorbent was immediately tested five times, and the adsorption capacities of PFOA onto the MIP in the adsorption–desorption–adsorption cycles are shown in Figure 12. After five adsorption–desorption–adsorption cycles, the uptake losses of PFOA were only approximately 8.09 and 3.77% for the 20 and 100 $\mu$g/L PFOA, respectively, compared to those in the first run. The results demonstrate that the MIP developed in this study has the potentiality to be reused without any decrease in its efficiency.

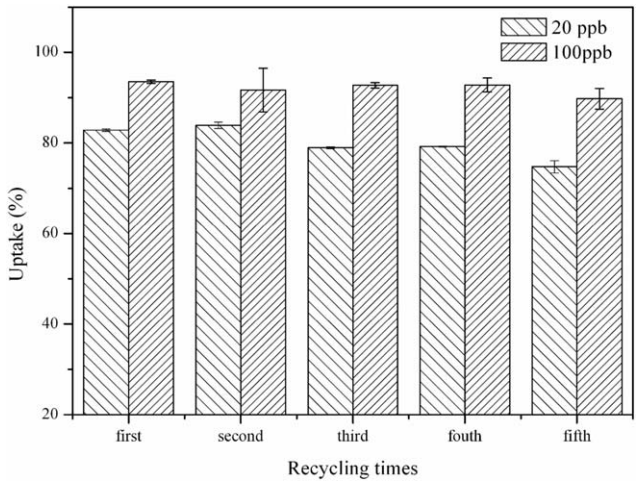


**Figure 12.** Uptake percentage of PFOA in the regeneration cycles for the MIP adsorbent.

## CONCLUSIONS

In this study, a PFOA–MIP adsorbent was successfully synthesized on the basis of a noncovalent molecular imprinting technique. The adsorption isotherms fit both the Langmuir and Freundlich model well; this indicated specific interaction, which was also confirmed by FTIR spectroscopy and NMR. The PFOA–MIP had a higher affinity for PFOA than the NIP did because of a favorable conformation. A high pH reduced the adsorption because of electrostatic repulsion, and a great ionic strength favored the adsorption through a reduction of the electrostatic repulsion. The PFOA–MIP had a higher recognition for PFOA than the PFCs did in competitive adsorption. Additionally, the PFOA–MIP had excellent reusability. All of the results indicate that the PFOA–MIP is a promising adsorbent for the selective removal of PFOA in aqueous environments.

## ACKNOWLEDGMENTS

The authors gratefully acknowledge the funding for this research provided by the National Natural Science Foundation of China (contract grant number 21177065) and the Tianjin Promoting Ocean by Science and Technology Project (contract grant number KJXH2012-22).

## REFERENCES

1. Moody, C. A.; Kwan, W. C.; Martin, J. W.; Muir, D. C.; Mabury, S. A. *Anal. Chem.* **2001**, *73*, 2200.
2. Moody, C. A.; Martin, J. W.; Kwan, W. C.; Muir, D. C.; Mabury, S. A. *Environ. Sci. Technol.* **2002**, *36*, 545.
3. Moody, C. A.; Field, J. A. *Environ. Sci. Technol.* **2000**, *34*, 3864.
4. Giesy, J. P.; Kannan, K. *Environ. Sci. Technol.* **2001**, *35*, 1339.
5. Giesy, J. P.; Kannan, K. *Environ. Sci. Technol. A* **2002**, *36*, 146.
6. Loos, R.; Locoro, G.; Huber, T.; Wollgast, J.; Christoph, E. H.; De Jager, A.; Manfred Gawlik, B.; Hanke, G.; Umlauf, G.; Zaldívar, J.-M. *Chemosphere* **2008**, *71*, 306.
7. Lindstrom, A. B.; Strynar, M. J.; Libelo, E. L. *Environ. Sci. Technol.* **2011**, *45*, 7954.
8. Wang, T.; Wang, Y.; Liao, C.; Cai, Y.; Jiang, G. *Environ. Sci. Technol.* **2009**, *43*, 5171.
9. Key, B. D.; Howell, R. D.; Criddle, C. S. *Environ. Sci. Technol.* **1997**, *31*, 2445.
10. Sinclair, E.; Kannan, K. *Environ. Sci. Technol.* **2006**, *40*, 1408.
11. Sun, H.; Li, F.; Zhang, T.; Zhang, X.; He, N.; Song, Q.; Zhao, L.; Sun, L.; Sun, T. *Water Res.* **2011**, *45*, 4483.

12. Murakami, M.; Kuroda, K.; Sato, N.; Fukushi, T.; Takizawa, S.; Takada, H. *Environ. Sci. Technol.* **2009**, *43*, 3480.
13. Skutlarek, D.; Exner, M.; Farber, H. *Environ. Sci. Pollut. Res. Int.* **2006**, *13*, 299.
14. Hansen, K.; Johnson, H.; Eldridge, J.; Butenhoff, J.; Dick, L. *Environ. Sci. Technol.* **2002**, *36*, 1681.
15. Loos, R.; Locoro, G.; Contini, S. *Water Res.* **2010**, *44*, 2325.
16. Zhao, L.; McCausland, P. K.; Folsom, P. W.; Wolstenholme, B. W.; Sun, H.; Wang, N.; Buck, R. C. *Chemosphere* **2013**, *92*, 464.
17. Sun, H.; Zhang, X.; Wang, L.; Zhang, T.; Li, F.; He, N.; Alder, A. C. *Environ. Sci. Pollut. Res.* **2012**, *19*, 1405.
18. Cai, Y.; Jiang, G.; Liu, J.; Zhou, Q. *Anal. Chem.* **2003**, *75*, 2517.
19. Jing, T.; Wang, J.; Liu, M.; Zhou, Y.; Zhou, Y.; Mei, S. *Environ. Sci. Technol.* **2014**, *21*, 1153.
20. Liu, Q.; Shi, J.; Zeng, L.; Wang, T.; Cai, Y.; Jiang, G. *J. Chromatogr. A* **2011**, *1218*, 197.
21. Haupt, K.; Mosbach, K. *Chem. Rev.* **2000**, *100*, 2495.
22. Whitcombe, M. J.; Chianella, I.; Larcombe, L.; Piletsky, S. A.; Noble, J.; Porter, R.; Horgan, A. *Chem. Soc. Rev.* **2011**, *40*, 1547.
23. Say, R.; Erdem, M.; Ersöz, A.; Türk, H.; Denizli, A. *Appl. Catal. A* **2005**, *286*, 221.
24. Lele, B.; Kulkarni, M.; Mashelkar, R. *React. Funct. Polym.* **1999**, *39*, 37.
25. Sellergren, B. Molecularly Imprinted Polymers: Man-Made Mimics of Antibodies and Their Application in Analytical Chemistry; Elsevier: Amsterdam, **2000**.
26. Ding, M.; Wu, X.; Yuan, L.; Wang, S.; Li, Y.; Wang, R.; Wen, T.; Du, S.; Zhou, X. *J. Hazard. Mater.* **2011**, *191*, 177.
27. Li, N.; Ng, T. B.; Wong, J. H.; Qiao, J. X.; Zhang, Y. N.; Zhou, R.; Chen, R. R.; Liu, F. *Food Chem.* **2013**, *139*, 1161.
28. Li, Y.; Li, X.; Chu, J.; Dong, C.; Qi, J.; Yuan, Y. *Environ. Pollut.* **2010**, *158*, 2317.
29. Lucci, P.; Núñez, O.; Galceran, M. *J. Chromatogr. A* **2011**, *1218*, 4828.
30. Xu, L.; Pan, J.; Dai, J.; Li, X.; Hang, H.; Cao, Z.; Yan, Y. *J. Hazard. Mater.* **2012**, *233*, 48.
31. Karoyo, A. H.; Wilson, L. D. *J. Colloid Interface Sci.* **2013**, *402*, 196.
32. Deng, S.; Shuai, D.; Yu, Q.; Huang, J.; Yu, G. *Front. Environ. Sci. Eng. China* **2009**, *3*, 171.
33. Yu, Q.; Deng, S.; Yu, G. *Water Res.* **2008**, *42*, 3089.
34. Ye, L.; Weiss, R.; Mosbach, K. *Macromolecules* **2000**, *33*, 8239.
35. Ho, Y.-S.; McKay, G. *Process Biochem.* **1999**, *34*, 451.
36. Ho, Y.; McKay, G. *Water Res.* **1999**, *33*, 578.
37. Hall, K.; Eagleton, L.; Acrivos, A.; Vermeulen, T. *Ind. Eng. Chem. Fundam.* **1966**, *5*, 212.
38. Yilmaz, E.; Mosbach, K.; Haupt, K. *Anal. Commun.* **1999**, *36*, 167.
39. Matsui, J.; Doblhoff-Dier, O.; Takeuchi, T. *Anal. Chim. Acta* **1997**, *343*, 1.
40. Kim, H.; Spivak, D. A. *J. Am. Chem. Soc.* **2003**, *125*, 11269.
41. Spivak, D. A. *Adv. Drug Delivery Rev.* **2005**, *57*, 1779.
42. Yoshimatsu, K.; Reimhult, K.; Krozer, A.; Mosbach, K.; Sode, K.; Ye, L. *Anal. Chim. Acta* **2007**, *584*, 112.
43. Kumar, K. V.; Sivanesan, S. *J. Hazard. Mater.* **2006**, *134*, 277.
44. Wu, W.; Sun, H. *Chemosphere* **2010**, *81*, 961.
45. Yang, Y.; Liu, X.; Guo, M.; Li, S.; Liu, W.; Xu, B. *Colloids Surf. A* **2011**, *377*, 379.
46. Burns, D. C.; Ellis, D. A.; Li, H.; McMurdo, C. J.; Webster, E. *Environ. Sci. Technol.* **2008**, *42*, 9283.
47. Yavuz, E.; Bayramoğlu, G.; Şenkal, B. F.; Arıca, M. Y. *J. Chromatogr. B* **2009**, *877*, 1479.
48. U.S. Environmental Protection Agency. Revised Draft Hazard Assessment of Perfluorooctanoic Acid and Its Salts; U.S. Environmental Protection Agency: Washington, DC, **2002**.
49. You, C.; Jia, C.; Pan, G. *Environ. Pollut.* **2010**, *158*, 1343.
50. Brooke, D.; Footitt, A.; Nwaogu, T. A. Environmental Risk Evaluation Report: Perfluorooctane Sulfonate (PFOS); UK Environment Agency: London, **2004**.